Comparison of intensity, transformation, and hybrid non-contrast CT ventilation methods for discriminating health from obstructive lung disease

William Clark[1,2], Ruth Hartley[2], Petr Novotny[2], Joshua R. Astley[1], Alberto M. Biancardi[1], Helen Marshall[1,4], Soniya Soniya[1], Sarah E. Gerard[3], Joseph M. Reinhardt[3], Christopher E. Brightling[2], Jim M. Wild[1,4], and Bilal A. Tahir[1,4]

[1] POLARIS, Division of Clinical Medicine, School of Medicine and Population Health, University of Sheffield, Sheffield, UK
[2] Institute for Lung Health, NIHR Leicester Biomedical Research Centre, University of Leicester, Leicester, UK
[3] Roy J. Carver Department of Biomedical Engineering, University of Iowa, Iowa, IA, USA
[4] Insigneo Institute for in Silico Medicine, University of Sheffield, Sheffield, UK
Wclark2@sheffield.ac.uk

Abstract. Non-contrast (NC) computed tomography (CT) ventilation imaging derives surrogates of regional lung function from paired inspiratory and expiratory breath-hold scans, avoiding the cost and complexity of contrast agents. Two method families dominate: intensity-based measures, which capture local density change but ignore volume change, and transformation-based (Jacobian) measures, which capture volume change. Hybrid measures combine both, but comparative evidence spanning health and obstructive disease is scarce, and healthy controls are largely absent from the NC CT validation literature. Here, we report an independent comparison of three conceptually distinct methods in a retrospective cohort of 254 subjects (143 asthma, 65 COPD, 46 healthy): intensity-based (HUVent), transformation-based (JacVent), and a two-compartment air-tissue hybrid (HybridVent) method. Using whole-lung mean ventilation as the primary biomarker, all three methods separated COPD from healthy subjects strongly (area under the curve, AUC, up to 0.94) and asthmatics with airway obstruction from healthy subjects moderately (AUC ≈ 0.77), but none differentiated asthma without airway obstruction from health. Mean ventilation correlated moderately with FEV_1/FVC and FEV_1 % predicted. At the whole-lung scale discrimination was largely indistinguishable between methods, although only the hybrid separated COPD both with and without spirometric obstruction from health. Lobar analysis showed only the hybrid's discrimination was lobe-dependent, separating COPD from health in the lower lobes (AUC up to 0.91) but not the upper.

Keywords: CT · Non-contrast functional imaging · Pulmonary function · Image Registration · Obstructive lung disease · CT Ventilation imaging

1 Introduction

Asthma and chronic obstructive pulmonary disease (COPD) are characterised by airflow obstruction, which is typically variable and reversible in asthma but fixed in COPD [1]. However, the distinction is not always clear, with substantial clinical overlap between severe asthma and COPD [2], motivating the need for tools that characterise the two diseases at a regional level. Computed tomography (CT) is widely used to visualise and quantify morphological abnormality such as air trapping and emphysema, but conventional structural CT does not directly report regional lung function, such as ventilation.

Modalities that employ exogenous contrast, such as single-photon emission CT [3], and hyperpolarised gas magnetic resonance imaging [4], image regional function but add cost and complexity through contrast production and specialised hardware. Non-contrast (NC) CT techniques instead derive functional surrogates from structural breath-hold images acquired routinely in clinical practice, with no contrast burden. Two principal families exist: intensity-based methods, which use voxel-to-voxel signal change between spatially aligned inflation states [5], and transformation-based methods, derived from the Jacobian determinant of the deformation field [6].

Each has complementary limitations: intensity-based methods neglect local volume change, while transformation-based methods neglect local compositional change. Hybrid methods combining both information sources, first formalised by Ding et al. [7], as the corrected Jacobian, address these limitations. We evaluate HybridVent, a hybrid surrogate based on a two-compartment air–tissue voxel model, which extracts a specific-ventilation surrogate from air-volume changes, incorporating local volume change through the Jacobian determinant. This corresponds to the corrected-Jacobian formulation of Ding et al. [7], originally termed specific air-volume change by corrected Jacobian (SACJ), implemented here within an ANTs registration pipeline.

Although NC functional CT has been assessed in asthma [8], COPD [9], and healthy versus asthmatic cohorts [10], large-cohort studies spanning health and obstructive lung disease remain limited, partly due to concerns over radiation exposure in health. This study compares three conceptually distinct NC CT ventilation methods, the intensity-based HUVent, the transformation-based JacVent, and HybridVent, across asthmatic, COPD and healthy cohorts. Our aim is to determine whether NC CT ventilation and derived measures can discriminate healthy lungs from obstructive lung disease.

2 Methods

2.1 Subjects and image acquisition

This study used a retrospective dataset previously described by Hartley et al. [11], comprising adults with COPD, asthma and healthy controls recruited at Glenfield Hospital, Leicester, UK. Diagnoses followed GOLD and GINA criteria [12, 13]; COPD patients had a smoking history >10 pack-years and were over 40 years of age. Non-contrast breath-hold CT was acquired at near total lung capacity (inspiration) and near

functional residual capacity (expiration) on a Siemens Sensation 16 scanner (120 kVp, 40 mAs, 16 × 0.75 mm collimation, B35f kernel, 0.75 mm isotropic). Asthmatic and COPD subjects were imaged within 60 minutes of salbutamol. Disease cohorts were further subdivided by FEV1/FVC z-score into normal FEV1/FVC ($z \geq -1.64$) and airway obstruction ($z < -1.64$) using Global Lung Function Initiative reference values [14].

2.2 Segmentation and registration

Lung parenchyma was segmented using a coarse-to-fine cascade of convolutional neural network [15, 16], utilizing a polymorphic learning strategy enabling training on diverse datasets and robust generalization to multiple lung disease phenotypes [17].

Image registration was performed using the Advanced Normalization Tools suite (ANTs) [18] in three sequential stages, based on Tahir et al. [8], with the expiratory breath-hold image as the fixed reference and the inspiratory image as the moving image. Prior to registration, lung segmentation masks were dilated by 8 voxels. After center-of-geometry initialization, rigid and affine transforms were applied using mutual information (32 bins, 25% sampling; gradient step 0.1) over a four-level pyramid (shrink factors 8, 4, 2, 1; sigmas 3, 2, 1, 0 voxels; ≤1000, 500, 250, 100 iterations). A deformable B-spline symmetric normalization transform (BSplineSyN; gradient step 0.2, mesh size 65) then used neighbourhood cross-correlation (radius 2) over a five-level pyramid (shrink factors 10, 6, 4, 2, 1; sigmas 5, 3, 2, 1, 0 voxels; ≤500, 200, 70, 50, 10 iterations). The registration produced both forward and inverse warps; the Jacobian determinant J, of the forward warp was computed for the transformation-based ventilation methods (JacVent and HybridVent).

2.3 Ventilation methods

Ventilation maps were computed from the registered inspiratory image and expiratory image, then voxel median filtered (radius 3) to reduce noise [19]. The intensity-based HU ventilation (HUVent) metric [5] is defined as:

$$\text{HUVent} = 1000 \times (\text{HU}_{\text{insp}} - \text{HU}_{\text{exp}}) / [\text{HU}_{\text{exp}} \times (1000 + \text{HU}_{\text{insp}})] \quad (1)$$

The transformation-based Jacobian ventilation (JacVent) metric [6] is derived from the determinant J(x) of the registration deformation field:

$$\text{JacVent} = J(x) - 1 \quad (1)$$

HybridVent reproduces the corrected-Jacobian measure (SACJ) of Ding et al. [7], expressed as air-fractions. Each voxel is modelled as a two-compartment mixture of air and tissue, such that $V^{\text{local}}=V^{\text{air}}+V^{\text{tissue}}$. Taking air ≤ −1000 HU, and tissue ≥ 0 HU [20], with the air fraction, $F^{\text{air}}= V^{\text{air}}/V^{\text{local}}$ calculated for both masked breath-hold images:

$$F^{\text{air}} = (\text{HU}^{\text{tissue}} - \text{HU}^{\text{local}}) / (\text{HU}^{\text{tissue}} - \text{HU}^{\text{air}}) \quad (1)$$

Since the Jacobian determinant J(x) represents the local volume ratio between inflation states, volumes of air at registered inspiration and expiration are:

$$V^{air}_{insp} = F^{air}_{insp} \times V^{local}_{insp} = F^{air}_{insp} \times J \times V^{local}_{exp} \quad \& \quad V^{air}_{exp} = F^{air}_{exp} \times V^{local}_{exp} \tag{1}$$

Substituting these into specific ventilation ($\Delta V^{air} / V^{air}_{at\ expiration}$), yields HybridVent:

$$\text{Hybrid Vent} = \frac{\Delta V^{air}}{V^{air}_{exp}} = \frac{V^{local}_{exp}\left(F^{air}_{insp} \times J - F^{air}_{exp}\right)}{F^{air}_{exp} \times V^{local}_{exp} + \varepsilon} = \frac{F^{air}_{insp} \times J - F^{air}_{exp}}{F^{air}_{exp} + \varepsilon} \tag{1}$$

Epsilon regularization ($\varepsilon = 0.00001$) was used to eliminate division by zeros. Equation 5 is algebraically identical to the SACJ measure of Ding et al. [7]

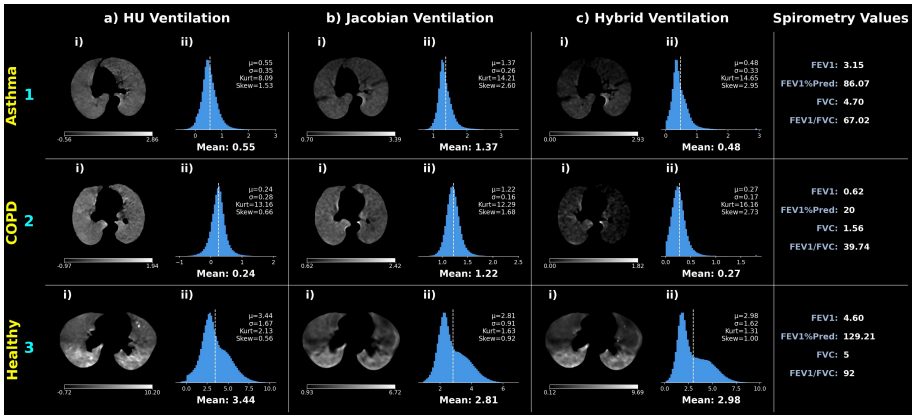

Fig. 1. Figures of a) HU-, b) Jacobian- and c) Hybrid- Ventilation for three subjects, Asthma [1], COPD [2], Healthy [3]. i) axial slice ventilation images with intensity range [0.1,99.9] percentiles, ii) intensity histogram-derived values, with mean (μ) indicated below. Subject's spirometric values, Forced expiratory volume in 1 second (FEV_1), FEV_1 % Predicted, Forced vital capacity (FVC) and FEV_1/FVC ratio shown.

2.4 Image analysis and statistics

For each ventilation map the primary biomarker was the whole-lung mean ventilation, which was derived alongside histogram-derived biomarkers (mean, skewness, kurtosis). Data normality was assessed by Shapiro-Wilk tests. Differences between primary cohorts, between health and normal- and abnormal (obstructed) subgroups, and all sub-groups were assessed with Kruskal–Wallis tests and Dunn's post-hoc comparisons. Paired group effect sizes r: (Small: $0.10 \leq r < 0.30$, Medium: $0.30 \leq r < 0.50$, Large: $r \geq 0.50$.). Discrimination of health from disease was quantified by the area under the receiver-operating-characteristic curve (AUC) with DeLong 95% confidence intervals (CI). Spearman correlations with Benjamini-Hochberg correction were computed between mean ventilation and spirometry (FEV1 % predicted, FEV1/FVC), with significant differences assessed by Meng's test. Analyses were performed in R 4.5.1, and a significance level of $p < 0.05$ was used for all tests. Lobar analysis was performed by repeating the histogram-derived biomarkers within each of the five pulmonary lobes.

3 Results

An overview figure for the three ventilation methods is shown in **Fig. 1**. Data was not normally distributed for any ventilation method (all p<0.0001). The dataset comprised 254 subjects: asthma (n = 143), COPD (n = 65) and healthy (n = 46).

3.1 Correlation with spirometry

Across the combined cohort correlation was moderate; against FEV_1%Pred and FEV_1/FVC, the highest were for HybridVent (r=0.524 and r=0.552 respectively), with 95% CI overlap with JacVent and HUVent. Correlation was stronger in COPD, with HybridVent FEV_1 % predicted correlation (r =0.708). Correlations were weaker in Asthma (|r| ≈ 0.21–0.33), and largely non-significant in health. Meng's test indicated differences between FEV_1%Pred, for JacVent and HybridVent in COPD (p=0.0252), and COPD-Abnormal (p=0.0396). For FEV_1/FVC, differences were significant between HUVent and HybridVent for all cohorts (0.0461), and Asthma (p=0.0243); all other comparisons were non-significant.

3.2 Disease-level discrimination

For mean ventilation, all three methods separated COPD from healthy subjects (all p<0.0001) and separated asthma from COPD (all p<0.0001). Asthma was separated from health modestly (all p=0.004). Effect sizes: COPD–healthy large (r = 0.70–0.75), asthma–COPD medium (r = 0.42–0.47), asthma–healthy small (r = 0.22). (**Fig. 2**).

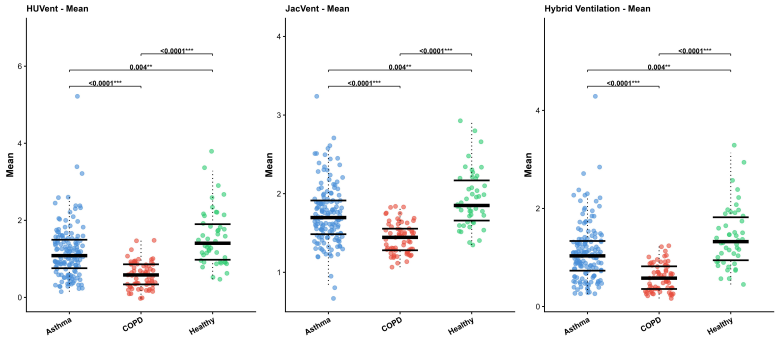

Fig. 1. Distribution plot for mean ventilation for HUVent, JacVent, and HybridVent for three cohorts, Asthma (n=143), COPD (n=65) and Healthy (n=46). Kruskal–Wallis with Dunn's significance indicated as * p<0.05, ** p<0.01, *** p<0.001.

3.3 Within-disease discrimination

Subdividing by FEV_1/FVC z-score for Asthma and COPD groups (**Fig. 3**) showed that COPD-Abnormal versus Healthy separation was robust (all p < 0.0001; r = 0.76–0.82), whereas COPD-Normal (n=10) versus Healthy (n=46) reached significance only for

HybridVent (p = 0.045). Asthma-Abnormal was separated from Healthy by all methods (all p < 0.0001) and from Asthma-Normal by all methods (HUVent p = 0.003, JacVent p = 0.001, HybridVent p = 0.001), while Asthma-Normal was not separable from Health (all p ≥ 0.08).

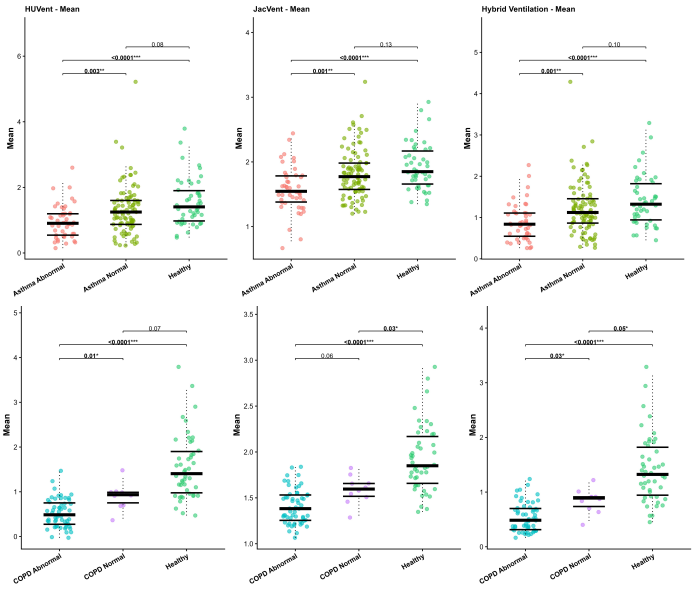

Fig. 3. Distribution plots for mean ventilation signal for HUVent, JacVent, and HybridVent for five cohorts, Asthma-Abnormal (n=46), Asthma-Normal (n=93), COPD–Abnormal (n=55), COPD-Normal (n=10) and Healthy (n=46). Kruskal-Wallis with Dunn's significance values shown, indicated as * p<0.05, ** p<0.01, *** p<0.001.

3.4 Discrimination performance (AUC)

Healthy versus COPD discrimination was uniformly high (HUVent 0.917, JacVent 0.903, HybridVent 0.914), rising for COPD-Abnormal (HUVent 0.938, HybridVent 0.931). Healthy-Asthma discrimination was weak (≈ 0.65), increasing to ≈ 0.77 for Asthma-Abnormal. Asthma-Normal was poorly separable from health (AUC ≤ 0.61) while COPD-Normal was moderate (AUCs >0.79). There were no significant differences in AUC's between ventilation methods at the disease-level (all p>0.05), except between HybridVent and JacVent for Healthy-COPD (p=0.026), and Healthy-COPD-Abnormal (p=0.016).

3.5 Lobar discrimination

Repeating the analysis within each lobe showed that the methods discriminated in different regions (Fig. 4). For mean ventilation, HybridVent separated COPD from health in the lower lobes (LLL AUC = 0.911, 95% CI 0.86–0.96; RLL 0.896, 0.84–

0.96) but not in the upper or middle lobes (0.59–0.61), whereas HUVent and JacVent showed the weaker, opposite pattern, with lower-lobe AUCs of 0.598 and 0.619 against 0.66–0.68 in the upper and middle lobes. Dunn's tests reflected the same asymmetry: HybridVent separated both COPD and asthma from health in the lower lobes only (all $p < 0.05$), with upper and middle lobes non-significant, whereas for HUVent and JacVent the strongest separations were in the upper and middle lobes ($p \leq 0.005$) and lower-lobe significance was inconsistent. For skewness and kurtosis the lower-lobe advantage was present for all three methods, with lower-lobe kurtosis discriminating COPD from health at AUC 0.78–0.88.

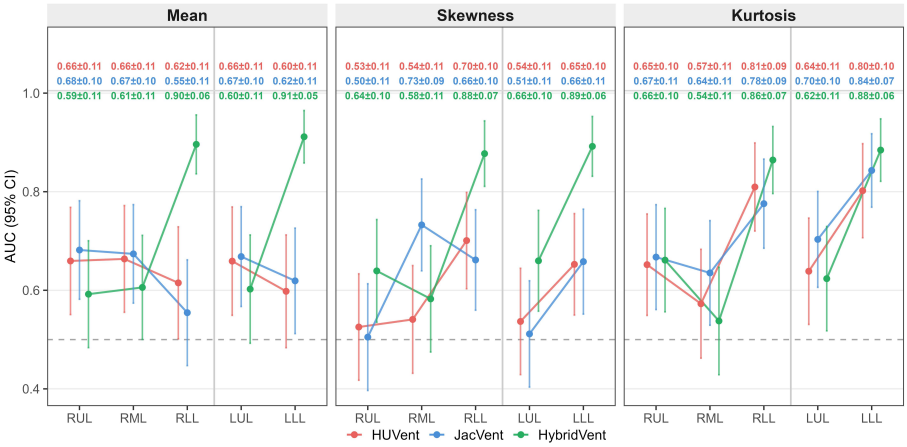

Fig. 4. AUC's for discriminating COPD from healthy subjects by lobe, for three histogram-derived biomarkers and three ventilation methods. Trend lines are drawn within each lung. Values above each point give the AUC ± DeLong 95% CIs.

4 Discussion

To our knowledge this is the first study to compare three conceptually distinct NC CT ventilation methods across healthy, asthmatic and COPD cohorts. Every method separated COPD from health very strongly at the whole-lung scale, demonstrating that the ventilation impairment of COPD is detectable irrespective of formulation. Discrimination was weaker in asthma and concentrated in the airway-obstructed subgroup; because imaging followed salbutamol, reversible obstruction would be reduced, plausibly attenuating the asthma–health separation and, to a lesser extent, the COPD–health separation, as bronchodilator responsiveness does not itself distinguish the two diseases [21]. Whole-lung differences between methods were minimal: HUVent and HybridVent never differed significantly on mean in any comparison, and only HybridVent separated all three of COPD-Abnormal, COPD-Normal and health. All methods correlated with FEV1%Pred and FEV1/FVC.

Because both JacVent and HybridVent inherit the Jacobian term, registration imprecision may propagate into the volume-correction and add spatial noise [22]. HU endpoints for air (−1000 HU) and tissue (0 HU) used by HUVent and HybridVent,

although consistent with prior work [5], may not be optimal: scanner calibration and reconstruction kernels affect HU distribution [23]. Improved registration and other intensity-deformation fusion strategies [24] are promising areas for improvement.

Our findings are broadly consistent with literature. Brennan et al. [25] reported HU-derived measures outperformed Jacobian-based ones in lung-cancer patients; Murphy et al. [26] and Cohen et al. [9] reported HUVent–FEV_1/FVC correlations of $r \approx 0.64$–0.74 in COPD, comparable to but somewhat higher than ours (HUVent $r = 0.618$ and HybridVent $r=0.608$ in COPD); and Bodduluri et al. [27] reported mean-Jacobian–FEV_1 $r = 0.60$ in 490 COPDGene subjects. Other Hybrid approaches [24] were shown to outperform other methods against contrast references.

Ding et al. compared the same three measures, against Xe-CT specific ventilation in mechanically ventilated sheep [7], finding the Hybrid Ventilation to be the most accurate (mean $r^2=0.82$ in 20-mm cubes), ahead of JacVent ($r^2=0.75$) and intensity ($r^2=0.58$) measures. Our cohort lacks an image reference and instead evaluates the measures against global spirometry and disease status, where the three performed comparably at the whole-lung level, and the HybridVent advantage was confined to a stronger FEV_1/FVC correlation, and the further separation of COPD cohorts.

The lobar analysis localised the differences between methods. HybridVent's separation of COPD from health was confined almost entirely to the lower lobes, whereas HUVent and JacVent discriminated most strongly in the upper and middle lobes. Whole-lung averaging therefore pools regions in which the methods behave differently, which may partly explain why they converge at the whole-lung scale, consistent with the scale dependence reported by Ding et al. between 20-mm and coarser sampling. This study has limitations, the primary of which is the lack of a regional function reference such as SPECT or hyperpolarised gas MRI against which the lobar gradients reported here could be validated. The COPD-Normal subgroup ($n = 10$) is likely too small for reliable statistical power within the COPD-obstruction subgroup analysis, and acquisition was single-centre, so multi-centre reproducibility of these results remains to be established.

5 Conclusion

In a large cohort spanning health, asthma and COPD, non-contrast CT ventilation derived from intensity, deformation and a corrected-Jacobian hybrid all discriminated COPD from health strongly and airway obstructed asthma from health moderately, using whole-lung mean ventilation. At the whole-lung scale the three methods performed similarly, although the hybrid uniquely separated COPD with and without airway obstruction from health. Lobar analysis showed that only the hybrid's discrimination was lobe-dependent, being confined to the lower lobes, indicating that whole-lung averaging obscures where the methods differ. This regional sensitivity supports the hybrid's potential as an obstruction-sensitive, contrast-free surrogate of regional lung function.

Disclosure of Interests. Joseph M. Reinhardt is a shareholder of VIDA Diagnostics, Inc. No other authors have competing interests to declare that are relevant to the content of this article.

6 References

1. Barnes, P.J.: Immunology of asthma and chronic obstructive pulmonary disease. Nat Rev Immunol. 8, 183–192 (2008).
2. Awad, M.T., Sankari, A.: Asthma and COPD Overlap. In: StatPearls. StatPearls Publishing, Treasure Island (FL) (2024).
3. Hopkins, S.R., Wielpütz, M.O., Kauczor, H.-U.: Imaging lung perfusion. J Appl Physiol (1985). 113, 328–339 (2012).
4. van Beek, E.J.R., Wild, J.M., Kauczor, H.-U., Schreiber, W., Mugler III, J.P., de Lange, E.E.: Functional MRI of the lung using hyperpolarized 3-helium gas. Journal of Magnetic Resonance Imaging. 20, 540–554 (2004).
5. Guerrero, T., Sanders, K., Castillo, E., Zhang, Y., Bidaut, L., Pan, T., Komaki, R.: Dynamic ventilation imaging from four-dimensional computed tomography. Phys Med Biol. 51, 777–791 (2006).
6. Reinhardt, J.M., Ding, K., Cao, K., Christensen, G.E., Hoffman, E.A., Bodas, S.V.: Registration-based estimates of local lung tissue expansion compared to xenon CT measures of specific ventilation. Med Image Anal. 12, 752–763 (2008).
7. Ding, K., Cao, K., Fuld, M.K., Du, K., Christensen, G.E., Hoffman, E.A., Reinhardt, J.M.: Comparison of image registration based measures of regional lung ventilation from dynamic spiral CT with Xe-CT. Medical Physics. 39, 5084–5098 (2012).
8. Tahir, B.A., Marshall, H., Hughes, P.J.C., Brightling, C.E., Collier, G., Ireland, R.H., Wild, J.M.: Comparison of CT ventilation imaging and hyperpolarised gas MRI: effects of breathing manoeuvre. Phys Med Biol. 64, 055013 (2019).
9. Cohen, J., Shekarnabi, M., Destors, M., Tamisier, R., Bouzon, S., Orkisz, M., Ferretti, G.R., Pépin, J.-L., Bayat, S.: Computed Tomography Registration-Derived Regional Ventilation Indices Compared to Global Lung Function Parameters in Patients With COPD. Front Physiol. 13, 862186 (2022).
10. Jahani, N., Choi, S., Choi, J., Haghighi, B., Hoffman, E.A., Comellas, A.P., Kline, J.N., Lin, C.-L.: A Four-Dimensional Computed Tomography Comparison of Healthy vs. Asthmatic Human Lungs. J Biomech. 56, 102–110 (2017).
11. Hartley, R.A., Barker, B.L., Newby, C., Pakkal, M., Baldi, S., Kajekar, R., Kay, R., Laurencin, M., Marshall, R.P., Sousa, A.R., Parmar, H., Siddiqui, S., Gupta, S., Brightling, C.E.: Relationship between lung function and quantitative computed tomographic parameters of airway remodeling, air trapping, and emphysema in patients with asthma and chronic obstructive pulmonary disease: A single-center study. Journal of Allergy and Clinical Immunology. 137, 1413-1422.e12 (2016).
12. Bateman, E.D., Hurd, S.S., Barnes, P.J., Bousquet, J., Drazen, J.M., FitzGerald, M., Gibson, P., Ohta, K., O'Byrne, P., Pedersen, S.E., Pizzichini, E., Sullivan, S.D., Wenzel, S.E., Zar, H.J.: Global strategy for asthma management and prevention: GINA executive summary. European Respiratory Journal. 31, 143–178 (2008).
13. Vestbo, J., Hurd, S.S., Agustí, A.G., Jones, P.W., Vogelmeier, C., Anzueto, A., Barnes, P.J., Fabbri, L.M., Martinez, F.J., Nishimura, M., Stockley, R.A., Sin, D.D., Rodriguez-Roisin, R.: Global Strategy for the Diagnosis, Management, and Prevention of Chronic Obstructive Pulmonary Disease. Am J Respir Crit Care Med. 187, 347–365 (2013).
14. Cooper, B.G., Stocks, J., Hall, G.L., Culver, B., Steenbruggen, I., Carter, K.W., Thompson, B.R., Graham, B.L., Miller, M.R., Ruppel, G., Henderson, J., Vaz Fragoso, C.A., Stanojevic, S.: The Global Lung Function Initiative (GLI) Network: bringing the world's respiratory reference values together. Breathe (Sheff). 13, e56–e64 (2017).

15. Gerard, S.E., Herrmann, J., Kaczka, D.W., Musch, G., Fernandez-Bustamante, A., Reinhardt, J.M.: Multi-resolution convolutional neural networks for fully automated segmentation of acutely injured lungs in multiple species. Medical Image Analysis. 60, 101592 (2020).
16. Gerard, S.E., Herrmann, J., Kaczka, D.W., Reinhardt, J.M.: Transfer Learning for Segmentation of Injured Lungs Using Coarse-to-Fine Convolutional Neural Networks. In: Stoyanov, D., Taylor, Z., Kainz, B., Maicas, G., Beichel, R.R., Martel, A., Maier-Hein, L., Bhatia, K., Vercauteren, T., Oktay, O., Carneiro, G., Bradley, A.P., Nascimento, J., Min, H., Brown, M.S., Jacobs, C., Lassen-Schmidt, B., Mori, K., Petersen, J., San José Estépar, R., Schmidt-Richberg, A., and Veiga, C. (eds.) Image Analysis for Moving Organ, Breast, and Thoracic Images. pp. 191–201. Springer International Publishing, Cham (2018).
17. Gerard, S.E., Herrmann, J., Xin, Y., Martin, K.T., Rezoagli, E., Ippolito, D., Bellani, G., Cereda, M., Guo, J., Hoffman, E.A., Kaczka, D.W., Reinhardt, J.M.: CT image segmentation for inflamed and fibrotic lungs using a multi-resolution convolutional neural network. Sci Rep. 11, 1455 (2021).
18. Avants, B.B., Tustison, N.J., Song, G., Cook, P.A., Klein, A., Gee, J.C.: A Reproducible Evaluation of ANTs Similarity Metric Performance in Brain Image Registration. Neuroimage. 54, 2033–2044 (2011).
19. Tahir, B.A., Hughes, P.J.C., Robinson, S.D., Marshall, H., Stewart, N.J., Norquay, G., Biancardi, A., Chan, H.-F., Collier, G.J., Hart, K.A., Swinscoe, J.A., Hatton, M.Q., Wild, J.M., Ireland, R.H.: Spatial Comparison of CT-Based Surrogates of Lung Ventilation With Hyperpolarized Helium-3 and Xenon-129 Gas MRI in Patients Undergoing Radiation Therapy. International Journal of Radiation Oncology*Biology*Physics. 102, 1276–1286 (2018).
20. Simon, B.A.: Non-Invasive Imaging of Regional Lung Function using X-Ray Computed Tomography. J Clin Monit Comput. 16, 433–442 (2000).
21. Beasley, R., Hughes, R., Agusti, A., Calverley, P., Chipps, B., del Olmo, R., Papi, A., Price, D., Reddel, H., Müllerová, H., Rapsomaniki, E.: Prevalence, Diagnostic Utility and Associated Characteristics of Bronchodilator Responsiveness. Am J Respir Crit Care Med. 209, 390–401 (2024).
22. Castillo, E., Castillo, R., Vinogradskiy, Y., Guerrero, T.: The numerical stability of transformation-based CT ventilation. Int J CARS. 12, 569–580 (2017).
23. Vergalasova, I., McKenna, M., Yue, N.J., Reyhan, M.: Impact of computed tomography (CT) reconstruction kernels on radiotherapy dose calculation. J Appl Clin Med Phys. 21, 178–186 (2020).
24. Tzitzimpasis, P., Ries, M., Raaymakers, B.W., Zachiu, C.: Hybrid method for estimating lung ventilation from CT by combining intensity and motion information. Med Phys. 52, 4528–4539 (2025).
25. Brennen, D., Schubert, L., Diot, Q., Castillo, R., Castillo, E., Guerrero, T., Martel, M.K., Linderman, D., Gaspar, L.E., Miften, M., Kavanagh, B.D., Vinogradskiy, Y.: Clinical validation of 4DCT-ventilation with pulmonary function test data. International journal of radiation oncology, biology, physics. 92, 423 (2015).
26. Murphy, K., Pluim, J.P.W., van Rikxoort, E.M., de Jong, P.A., de Hoop, B., Gietema, H.A., Mets, O., de Bruijne, M., Lo, P., Prokop, M., Ginneken, B. van: Toward automatic regional analysis of pulmonary function using inspiration and expiration thoracic CT. Medical Physics. 39, 1650–1662 (2012).
27. Bodduluri, S., Bhatt, S.P., Hoffman, E.A., Newell, J.D., Martinez, C.H., Dransfield, M.T., Han, M.K., Reinhardt, J.M., COPDGene Investigators: Biomechanical CT metrics are associated with patient outcomes in COPD. Thorax. 72, 409–414 (2017).